RAPID COMMUNICATIONS

PHYSICAL REVIEW B VOLUME 52, NUMBER 8 15 AUGUST 1995-II

Excitons in a II-VI semiconductor microcavity in the strong-coupling regime

P. Kelkar, V. Kozlov, H. Jeon, and A. V. Nurmikko
Division of Engineering and Department of Physics, Brown University, Providence, Rhode Island 02912

C.-C. Chu, D. C. Grillo, J. Han, C. G. Hua, and R. L. Gunshor
School of Electrical Engineering, Purdue University, West Lafayette, Indiana 47907
(Received 25 May 1995)

Microcavities which contain Zn-Cd-Se quantum wells as the resonant medium have been fabricated and tested at blue-green wavelengths. We see clear evidence of coupled-mode behavior at the $n=1$ heavy-hole exciton in both angle and temperature tuning experiments, with anticrossing (vacuum-Rabi) splittings approaching 20 meV. The exciton-cavity interaction is consistent with predictions by theory in the strong-coupling regime, and illustrates the impact of the large oscillator strength available in II-VI compounds.

Excitons in semiconductor microcavities is a contemporary subject as illustrated by several recent experimental reports that demonstrate the impact of enhanced coupling between extended electronic states in a crystalline solid and resonant electromagnetic waves.[1–5] Important related theoretical activity has also emerged, ranging from classical reinterpretation of atomic physics pheonomena to full quantum description of the exciton-polariton states in a microcavity.[5–9] Both experiment and theory have concentrated on the GaAs-based semiconductor heterostructures, in large part due to ready access by experiment to quality epitaxial material. Driven by the prospects of new compact blue-green diode lasers and other optoelectronic applications at short visible wavelengths, strong recent progress has been witnessed in wide-gap II-VI semiconductors, and a range of heterostructure designs is now available to test ideas associated with microcavity effects. One important and motivating difference, in this connection, between the GaAs- and ZnSe-based quantum-well systems is that a considerably larger oscillator strength can be obtained in the latter case, as well as the condition where the exciton binding energy satisfies the inequality $E_x > \hbar\omega_{LO}$, kT (where $h\omega_{LO}$ is the optical phonon energy and kT is evaluated at room temperature).[10] The robustness of such quasi-two-dimensional (2D) excitons in II-VI heterostructures is of relevance to the new blue-green light emitters; here we demonstrate their impact in a microcavity environment in initial experiments. We use both angle tuning and temperature tuning to show coupled-mode behavior between the $n=1$ heavy-hole (HH) exciton in a (Zn,Cd)Se quantum well (QW) and the microcavity electromagnetic modes to obtain a quantitative measure of the normal mode (vacuum-Rabi) splitting. The splittings can reach values approaching 20 meV, and are clearly discernible in spite of a background line broadening on the order of 10 meV. Semiclassical theory provides very good agreement with the experiments in which transmission, reflectance, and photoluminescence have been used as optical probes.

The II-VI semiconductor optical structure was based on a pseudomorphic (Zn,Cd)Se/Zn(S,Se)/(Zn,Mg)(S,Se) separate confinement heterostructure design, in which three uniformly strained 75-Å-thick $Zn_{1-x}Cd_xSe$ QW's provided the quasi-2D exciton confinement ($x_{Cd}=0.24$), cladded by Zn(S,Se) ($L \approx 2\times 690$ Å) and (Zn,Mg)(S,Se) ($L \approx 2\times 1830$ Å) inner and outer confinement layers, all grown by molecular-beam epitaxy. Figure 1(a) shows the schematic of this heterostructure in the form of a simplified band diagram. The sulfur concentration was approximately $y \approx 0.07$ in the ternary ZnS_ySe_{1-y} and $y' \approx 0.12$ in the

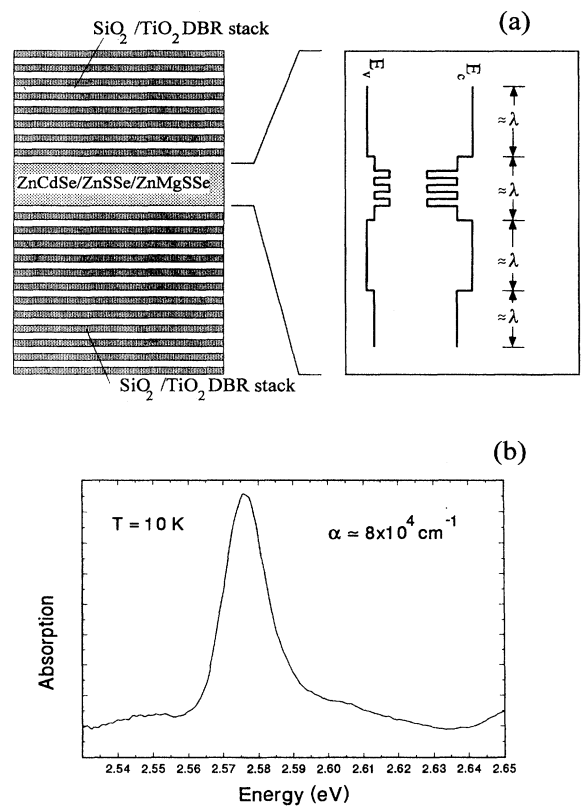

FIG. 1. (a) Schematic of the microcavity structure, including the energy-band diagram of the II-VI heterostructure. (b) Portion of the absorption spectrum of the as-grown material at $T=10$ K displaying the $n=1$ HH exciton absorption resonance of the three 75-Å-thick (Zn,Cd)Se QW's.

 © 1995 The American Physical Society

$Zn_{1-z}Mg_zS_{y'}Se_{1-y'}$ quaternary layer; the Mg concentration in the latter was $z \approx 0.09$. An additional spacer layer of Zn(S,Se) ($L \approx 1790$ Å) was included to complete an approximately 4λ-thick II-VI semiconductor cavity near the $n=1$ HH QW exciton resonance, with the QW's located spatially at one antinode position of the optical standing wave. Except for the QW's, the compositions of the ternary and quaternary layers were nominally lattice matched to the III-V buffer/substrate, which also contained a homoepitaxially grown (Al,Ga)As etch stop layer. Figure 1(b) displays the absorption spectrum of the (Zn,Cd)Se QW near the $n=1$ HH exciton at $T=10$ K showing a well-defined, spectrally isolated resonance. The approximately 10-meV exciton linewidth is due to alloy potential fluctuations (compositional disorder) and gives a measure of the inhomogeneous broadening of this resonance. The peak value for the absorption coefficient $\alpha \approx 8 \times 10^4$ cm^{-1} corresponds to an oscillator strength of about $f \approx 1 \times 10^{13}$ cm^2 per QW. The low-temperature excitonic band gaps for the Zn(S,Se) and (Zn,Mg)(S,Se) barrier/confinement layers were approximately 2.85 and 3.04 eV, respectively.

To complete the microcavity structure, we employed reactive ion-beam sputter deposition of dielectric SiO_2/TiO_2 stacks to form the distributed Bragg reflectors (DBR's). The III-V material was removed selectively by wet etching to open windows for growing of the bottom reflector. Due to the relatively large inhomogeneous broadening of the $n=1$ HH exciton in the as-grown material, as well as the homogeneous broadening at higher temperatures (see below), we chose a moderate reflectivity for the mirrors ($R \approx 0.995$), which could be obtained by depositing five SiO_2/TiO_2 layer pairs. Optical characterization measurements in transmission or reflection at a cavity mode well below the exciton resonance indicated a "cold" cavity linewidth $\Delta \nu_c = 4$ meV, or a value for the quality factor of approximately $Q \approx 650$. Similar structures, although with considerably higher Q factors, have been fabricated by us recently to demonstrate optically pumped vertical cavity surface emitting laser operation in the blue green.[11]

The microcavity effects at a fixed temperature were investigated while using angle tuning of a transmission probe to vary the frequency difference between the exciton and the cavity resonance. Figure 2 shows the transmission spectrum at $T=50$ K as a function of the external angle of incidence θ, measured with respect to the normal to the sample surface. Angular spreading was minimized by restricting the transmitted radiation from a white-light source by apertures to a small solid angle ($\Delta\theta < 1°$). The temperature was chosen such that the range for angle tuning would access the physically interesting regime of the exciton-electromagnetic wave interaction, given the initial spectral location of the cavity mode on the low-energy side of the QW exciton. At this temperature, the homogeneous contribution to the linewidth is estimated to be approximately 2 meV, and is due to acoustic deformation potential and piezoelectric scattering.[10] The emergence of a distinct splitting with increasing angle is quite evident in the figure as the cavity mode approaches the exciton resonance; Fig. 3 highlights this interaction further by showing the details of the spectrum at an angle $\theta = 26°$. Note that the minimum splitting at closest approach of the mixed exciton-cavity mode is $\Omega \approx 17.5$ meV. This value not only exceeds the substantial inhomogeneous linewidth in the (Zn,Cd)Se QW's but is also a sizable fraction of the HH exciton binding energy (determined to be approximately 40 meV from previous work on samples with similar QW parameters[10]).

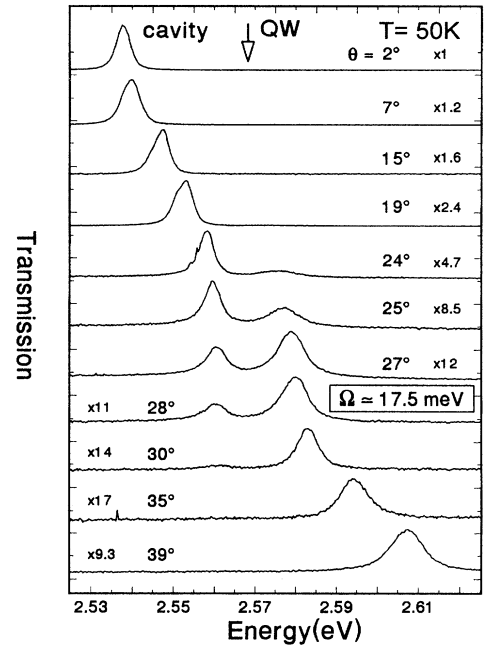

FIG. 2. Transmission spectrum of the microcavity at $T=50$ K as a function of the angle of incidence θ near the $n=1$ HH exciton resonance. The scaling amplitude factors are included.

In modeling the data in Figs. 3 and 4, we have used the results of the work by Savona *et al.*,[7] in which results from a nonlocal, semiclassical approach gives ready access for comparing experiment with theory. The model is specifically applied to the strong-coupling regime, where the interaction energy (vacuum-Rabi frequency) exceeds the cavity and exciton linewidths. The dashed line in Fig. 3 is a fit from the theory in which Lorentzian line shapes were used for the cavity and exciton resonances; while the energy positions for the mixed mode (peak positions) are in good agreement, the experimental linewidths are broader. The positions of the ob-

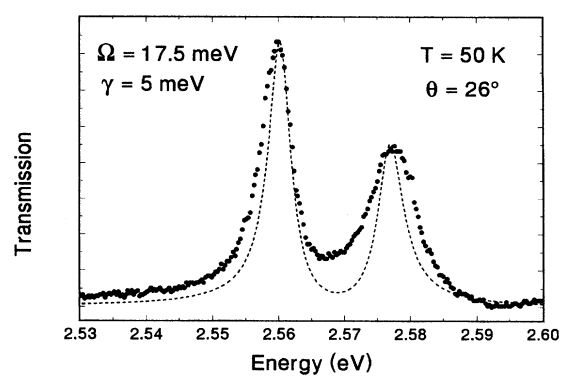

FIG. 3. Transmission spectrum at $T=50$ K at an angle of $\theta = 26°$. The dashed line is a result of the model as discussed in the text.

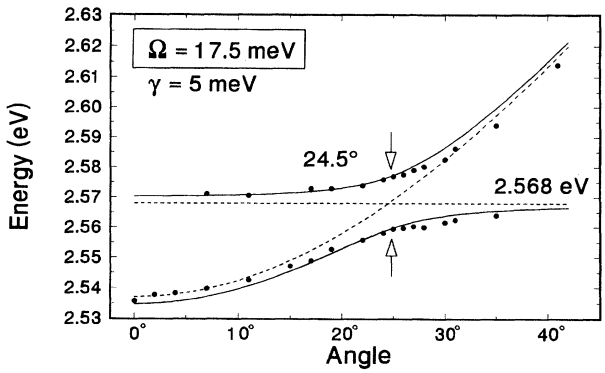

FIG. 4. The comparison between experiment (points) and theory (solid lines) in the strong-coupling regime according to the model discussed in the text. The dashed line shows the energies of the uncoupled exciton and cavity resonances.

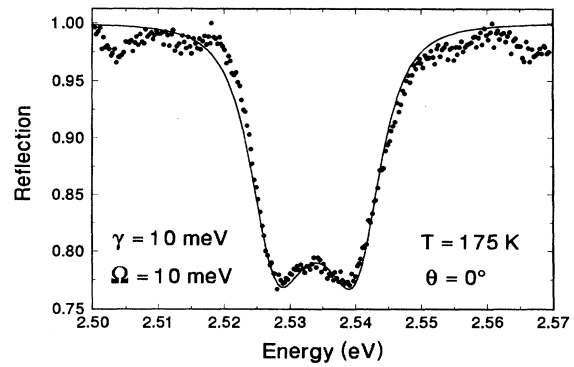

FIG. 5. Reflectance spectrum at normal incidence from a (Zn,Cd)Se QW microcavity at $T=175$ K. The solid line is from a calculation as indicated in the text.

served peak photon energies in the transmission data of Fig. 2 are summarized in Fig. 4 (circles), together with the results from the model calculation (solid lines), where the angle tuning only enters into the cavity frequency $\omega_m(\theta)$ (corrected for Fresnel refraction). The following parameters were used in obtaining the fit to the experimental data in both Figs. 3 and 4: mirror reflectivity $R=0.994$, cavity linewidth $\gamma_c=c(1-R)/(2n_{\mathrm{cav}}L_{\mathrm{eff}})=2.1$ meV, nonradiative broadening $\gamma=5.0$ meV (halfwidth at half maximum in the notation of Ref. 7), and the "radiative linewidth" of the exciton $\hbar\Gamma_0=0.3$ meV for the total three QW's. The "bare" exciton resonance was fixed at $E_x=2.568$ eV and an effective index of refraction $n_{\mathrm{cav}}=2.68$ was used. The index is close to a measured value for (Zn,Mg)(S,Se), the thickness of which dominates the total optical path length of the microcavity. The effective cavity length L_{eff} was obtained from measurements by transmission electron microscope of the II-VI layer thickness and by calculating the contribution by the SiO_2/TiO_2 DBR stacks from multilayer theory. In terms of the notation in Ref. 7, the fit yields a value for the interaction matrix element $V\approx 8$ meV [the quantity V is proportional to $V\sim(\Gamma_0/n_{\mathrm{cav}}L_{\mathrm{eff}})^{1/2}$]. The values for both V and the Rabi-splitting Ω reflect directly the large exciton oscillator strength in a widegap II-VI semiconductor microcavity. We note that the use of the inhomogeneous linewidth (half width in the notation for γ) as the "nonradiative" broadening parameter appears to be an intuitively correct physical choice (as opposed to the homogeneous broadening), given the strong interaction regime ($\Omega>\gamma_{\mathrm{inh}}>\gamma_{\mathrm{hom}}$) in which the vacuum-Rabi oscillations in effect couple the distribution of excitonic oscillators across the entire resonance. The argument is qualitative at best, however, and we have not attempted, in the present work, to investigate any further the implications of a substantial inhomogeneous broadening on the model.

We have also varied the sample temperature to obtain another means for continuous tuning of the frequency difference between the exciton and the cavity resonance (from the band-gap shift dE_g/dT), similar to the approach employed in Ref. 5. The circumstances are now more complex, since several key experimental parameters (such as γ, γ_c, and $\hbar\Gamma_0$) can be temperature dependent. Nonetheless, clear evidence for normal mode interaction could be observed in both reflectance and photoluminescence experiments. As an example, Fig. 5 shows the white light reflectance spectrum at $T=175$ K at normal incidence for the same structure, where the vacuum-Rabi splitting behavior is again manifested, in spite of the increased spectral broadening. The solid line through the data points is obtained from the model described above in which the contribution by exciton-LO phonon scattering[10] has been accounted for by an increase of the nonradiative broadening to $\gamma=10$ meV (half width at half maximum). The increase in the scattering rate reduces the value of Ω to approximately 10 meV in Fig. 5. Similar observations were made when recording photoluminescence spectra, and, while not showing the details of the data in this paper, we reached a good agreement with a classical coupled oscillator model for the observed spectral positions of normal modes in both temperature-tuned reflection and luminescence experiments.

In summary, we have shown the feasibility of fabricating a II-VI semiconductor microcavity in which the exciton-electromagnetic field interaction leads to pronounced normal-mode (vacuum-Rabi) splittings. These early results are encouraging since considerable variation is possible within the II-VI heterostructures for design of the exciton system for the study of other consequences of the strong-coupling effects.

This research was supported by the National Science Foundation (at Brown, DMR-9121747; at Purdue, DMR-9202957), ARPA (Contract No. DMC/MDA972-93-2-0013), and AFOSR (F49620-92-J-0440).

[1] Y. Yamamoto, S. Machida, and G. Bjork, Phys. Rev. A **44**, 657 (1991).

[2] T. Yamauchi, Y. Arakawa, and M. Nishioka, Appl. Phys. Lett. **58**, 2339 (1991).

[3] C. Weisbuch, M. Nishioka, A. Ishikawa, and Y. Arakawa, Phys. Rev. Lett. **69**, 3314 (1992).

[4] R. Houdre, C. Weisbuch, R. P. Stanley, U. Oesterle, P. Pellandini, and M. Ilgems, Phys. Rev. Lett. **73**, 2043 (1994).

[5] T. A. Fisher, A. M. Afshar, D. M. Whittaker, M. S. Skolnick, J. S. Roberts, G. Hill, and M. A. Pate, Phys. Rev. B **51**, 2600 (1995).

[6] D. S. Citrin, IEEE J. Quantum Electron. **30**, 997 (1994).

[7] V. Savona, L. C. Andreani, P. Schwendimann, and A. Quattopani,

Solid State Commun. **93**, 733 (1995); V. Savona, Z. Hradil, A. Quattopani, and P. Schwendimann, Phys. Rev. B **49**, 8774 (1994).

[8] S. Pau, G. Bjork, J. Jacobson, H. Cao, and Y. Yamamoto, Phys. Rev. B **51**, 7090 (1995).

[9] S. Jorda, Phys. Rev. B **51**, 10 185 (1995).

[10] N. T. Pelekanos, J. Ding, M. Hagerott, A. V. Nurmikko, H. Luo, N. Samarth, and J. Furdyna, Phys. Rev. B **45**, 6037 (1992).

[11] H. Jeon, V. Kozlov, P. Kelkar, A. V. Nurmikko, D. C. Grillo, J. Han, M. Ringle, and R. L. Gunshor, Electron. Lett. **31**, 106 (1995); (unpublished).